



GLOBAL JOURNAL OF RESEARCHES IN ENGINEERING  
CIVIL AND STRUCTURAL ENGINEERING  
Volume 13 Issue 3 Version 1.0 Year 2013  
Type: Double Blind Peer Reviewed International Research Journal  
Publisher: Global Journals Inc. (USA)  
Online ISSN: 2249-4596 & Print ISSN: 0975-5861

## Boundary Element Analysis of Pile Groups in Sand

By Mohammed Y. Fattah, Kais T. Shlash & Madhat S. Al-Soud

*University of Technology, Baghdad, Iraq*

**Abstract** - This paper is devoted to make use of the boundary element method as a practical problem solving tool to analyze the soilpile interaction problems. A computer program was adopted for the analysis process. It is a computer package called PGroupN which is concerned mainly with the analysis of the pile group problems. A non-linear soil model has been adopted with this program to assess the pile-soil interaction within the group. Some parametric studies were carried out with this problem including the pile diameter, pile length, spacing to diameter ratio, soil type (sand) and the thickness of stratum.

It was found that for 9 pile group analyzed, the corner pile carries about 4% more than the average load, while the border and the center piles carry 2% and 10% less than the average load, respectively. As the ratio of pile spacing to diameter (S/D) increases, the difference between loads on each pile decreases, especially between the corner and the center piles.

**Keywords** : *boundary element, pile group, sand, pile load.*

**GJRE Classification** : *FOR Code: 650104, 961499*



*Strictly as per the compliance and regulations of :*



# Boundary Element Analysis of Pile Groups in Sand

Mohammed Y. Fattah <sup>α</sup>, Kais T. Shlash <sup>σ</sup> & Madhat S. Al-Soud <sup>ρ</sup>

**Abstract** - This paper is devoted to make use of the boundary element method as a practical problem solving tool to analyze the soil- pile interaction problems. A computer program was adopted for the analysis process. It is a computer package called PGroupN which is concerned mainly with the analysis of the pile group problems. A non-linear soil model has been adopted with this program to assess the pile-soil interaction within the group. Some parametric studies were carried out with this problem including the pile diameter, pile length, spacing to diameter ratio, soil type (sand) and the thickness of stratum.

It was found that for 9 pile group analyzed, the corner pile carries about 4% more than the average load, while the border and the center piles carry 2% and 10% less than the average load, respectively. As the ratio of pile spacing to diameter (S/D) increases, the difference between loads on each pile decreases, especially between the corner and the center piles.

**Keywords** : boundary element, pile group, sand, pile load.

## 1. BOUNDARY ELEMENT TECHNIQUE

While the finite element calculations constitute the major part of the computer studies and considered the most popular technique, the boundary element method (BEM) has been well examined as complementary or alternative system of analysis, with a view of reduce program running costs and enabling larger problems to be tackled.

The BEM is a boundary integral equation technique. The problem boundaries are discretized so that a singular solution of the governing differential equation can be integrated around them, yielding an appropriate source distribution which will generate the specified boundary conditions. Alternatively, the method may be regarded as a 'super' finite element technique, where each element models a homogenous zone (Hobbs et al., 1978).

Early attempts at employing numerical solution procedures for the solution of boundary integral equations have developed into two distinct and parallel ways. One of these is an intuitive, physical approach and the other is a more mathematical treatment based on concepts of classical potential theory (Banerjee and

Butterfield, 1981) (Crouch and Starfield, 1983) (Venturini, 1983), (Beer, 1986) and (Beer and Watson, 1992).

### a) Boundary Element Method in pile-soil Interaction Problems

Poulos (1971a) proposed integral equations for an elastic solution of laterally loaded pile. This problem is based on Mindlin's solution (Mindlin, 1936) for a point load in a homogeneous, isotropic elastic half space. The pile response shown in Figure 1 was calculated by integrating Mindlin's equation over the corresponding area of the soil. In Figure 1a, the pile is discretized into a number of elements. The transition of load through the pile is shown in Figure 1b, while the pile deformation ( $w$ ) is shown in Figure 1c. The method could be extended to study the behavior of pile groups (Poulos, 1971b).

The integral equation mentioned above, was extended by Butterfield and Banerjee (1971b) using a BEM to treat a soil continuum and pile as two separate domains whose boundaries were discretized into a finite number of elements. A set of fictitious tractions were assumed at the pile – soil interface. It had been shown by Butterfield and Banerjee (1971b) that these fictitious tractions were identical to the real ones for pile slenderness ratio greater than five. Each boundary element was associated with known tractions and displacements. Some of these were known over parts of the boundary, the rest of them were computed using Kelvin' solutions (Lancellotta, 2009). Once these boundary values were obtained, the displacements and tractions at any point inside the domain could be computed.

Butterfield and Banerjee (1971a) presented an elastic analysis for the general compressible pile group problem including a rigid smooth ground contacting cap. The problems were formulated as an integral equation developed from Mindlin's analysis (Mindlin, 1936) for a point load embedded within a semi-infinite ideal elastic half space. By distributing such point loads over the pile cap – supporting medium interface and the pile shaft and pile base – medium interface, an integral representation was obtained given the vertical displacement at all points in the medium in terms of fictitious stress intensities.

Chin (2004) derived elastic design charts for axial pile settlement response from the elastic response simplified BEM for piles imbedded in a two-layer soil

Author <sup>α</sup> <sup>σ</sup> : Building and Construction Eng. Dept., University of Technology, Baghdad, Iraq. E-mail : myf\_1968@yahoo.com

Author <sup>ρ</sup> : Civil Eng. Dept., College of Engineering, University of Mustansiriyah, Iraq.

continuum. These charts cover the practical ranges of pile and soil parameters as shown in Figure 2:

*b) Application of the Boundary Element Method to Soil-Pile Interaction Problems*

This paper presents the results of a numerical analysis for the solution of soil-pile interaction problems using the BEM.

A problem was chosen to investigate the behavior during the variation of different parameters. A summary of the analysis procedure is presented here followed by a comprehensive discussion to all the obtained results in order to evaluate the work, as much as possible, according to the adopted researches.

Because of the particulate nature of the mineral skeleton of the soil, the stress-strain behavior of the soil is exceedingly complex. One way out from this complexity is to use concepts and formulas from the theory of elasticity. This means that the actual non-linear behavior of soil is linearized which may lead to a conservative design. Thus, the non-linearity represents the realistic behavior of the soil and it is adequate to simulate its general problems.

Many researchers emphasized the importance of considering soil non-linearity in routine design. For pile group problems, this issue has not been satisfactorily addressed yet, and current design practice is still generally based on linear approaches (Basile, 2003). The main drawback to the application of linear models to pile group problems is that they ignore the non-linear load-deformation characteristics of soil and hence misrepresent the force in piles, specifically by giving higher stresses in group corners. The cost of this in practice is high and there is an urgent need in industry for efficient non-linear analysis method (Basile, 2003).

A reasonable compromise between excessive complexity and unacceptable simplicity is provided by the BEM, in which the pile-soil interface is discretized and the characteristics of soil response are represented in a lumped form by ascribing the behavioral features of the soil to the interface elements (Poulos, 1989).

## II. METHOD OF ANALYSIS

The analysis with the program PGroupN is based on complete non-linear BEM formulation. The analysis involves discretization of only the pile-soil interface into a number of cylindrical elements, while the base is represented by a circular (disc) element. The method employs a subtracting technique in which the piles and the surrounding soil are considered separately and then compatibility and equilibrium conditions are imposed at the interface.

The external load is applied incrementally and, at each increment, a check is made that the stress state at the pile-soil interfaces does not violate the yield criteria. This is achieved by specifying the limiting

stresses of the soil for the axial pile shaft capacity, and end-bearing resistance. The elements of the pile-soil interface which have yielded can take no additional load and any increase in load is therefore redistributed between the remaining elements until all elements have failed. Thus, by successive application of loading increments, the entire load-displacement relationship for the pile group is determined.

*a) BEM Program PGroupN*

Repute calculation engine is the leading-edge program PGroupN which provides a complete 3D non-linear boundary element solution of the soil continuum. This overcomes limitations of traditional interaction-factor methods and gives more realistic predictions of deformations and the load distribution between piles (Basile, 2003).

This program is based on a complete boundary element formulation extending an idea first proposed by Butterfield and Banerjee (1971, a). The method employs a substructuring technique in which the piles and the surrounding soil are considered separately and then compatibility and equilibrium conditions are imposed at the interface. Given unit boundary conditions, i.e. pile group loads and moments; these equations are solved, thereby leading to the distribution of stresses, loads and moments in the piles for any loading condition (Geocentrix Ltd, 2002).

*b) Choice of Soil Parameters*

The choice of soil parameters for PGroupN is simple and direct: for a linear analysis, it is only necessary to define two soil parameters whose physical interpretation is clear, i.e. the soil modulus ( $E$ ) and Poisson's ratio ( $\nu$ ). If the effects of soil non-linearity are considered in elastic-plastic analysis, the strength properties of soil need also to be specified, i.e. the undrained shear strength ( $c_u$ ) for cohesive soils and the angle of friction ( $\phi$ ) for cohesionless soils. Thus the applied method, by taking into account the continuous nature of pile-soil interaction, removes the uncertainty of  $t-z$  and  $p-y$  approaches and provides a simple design tool based on conventional soil parameters (Basile, 2003).

*c) Nonlinear Soil Model*

Soil is not a linear material. The relations between stress and strain are much more complicated than the simple, linear elastic material. Therefore, in order to represent geotechnical problems realistically, some form of nonlinear relation must be used (Christian and Desai, 1977).

The widely used function for simulation of stress-strain curves in the finite element analysis was formulated by Chang and Duncan (1970), and Duncan and Chang (1970) using Kondner's (1963) finding that the plot of stress versus strain in a triaxial compression

test is very nearly a hyperbola. Figure 3 illustrates such relation, which can be stated in equation form:

$$\sigma = \frac{\varepsilon}{b + a\varepsilon} \tag{1}$$

or

$$\frac{\varepsilon}{\sigma} = b + a\varepsilon \tag{2}$$

In these equations, the subscripts have been removed from the stresses and strains for clarity, so that  $\sigma$  and  $\varepsilon$  represent vertical stress and strain, respectively. The latter form of the equation plots as a straight line (Figure 4) and, conversely, a plot with axis  $\varepsilon/\sigma$  and  $\varepsilon$  can be used to check whether the data from a test do fit a hyperbola or to find the parameters of the hyperbola from the test data.

To find the tangent modulus, it is first helpful to observe that at very small strains:

$$\sigma = \frac{\varepsilon}{b} \tag{3}$$

So that  $1/b$  is the initial Young's modulus  $E$ . At large strains, the relation becomes:

$$\sigma = \frac{1}{a} \tag{4}$$

So that  $1/a$  is the compressive strength; actually,  $1/a$  is the asymptote. Since the compressive strength will be reached before the curve becomes asymptotic as shown in Figure 2, it is customary to require the compressive strength  $s$  to be  $R_f/a$ , where  $R_f$  is the failure ratio. Thus

$$a = \frac{R_f}{s} \tag{5}$$

Equation (1) can also be solved for  $\varepsilon$ :

$$\varepsilon = \frac{b\sigma}{1 - a\sigma} \tag{6}$$

The tangent modulus at any level of stress or strain is:

$$E_t = \frac{\partial\sigma}{\partial\varepsilon} = \frac{b}{(b + a\varepsilon)^2} = \frac{1}{b}(1 - a\sigma)^2 = E_i \left(1 - \frac{R_f\sigma}{s}\right)^2 \tag{7}$$

For a Mohr-Coulomb material at failure:

$$(\sigma_1 - \sigma_3)_f = \frac{2\sigma_3 \sin\phi + 2c \cos\phi}{1 - \sin\phi} \tag{8}$$

The term  $\sigma/s$  is the ratio between the existing  $\sigma_1 - \sigma_3$  and  $s$  that would be available for the existing  $\sigma_3$ . The ratio is:

$$\frac{\sigma}{s} = \frac{(\sigma_1 - \sigma_3)(1 - \sin\phi)}{2\sigma_3 \sin\phi + 2c \cos\phi} \tag{9}$$

The tangent modulus now becomes:

$$E_t = E_i \left[1 - \frac{R_f(\sigma_1 - \sigma_3)(1 - \sin\phi)}{2\sigma_3 \sin\phi + 2c \cos\phi}\right]^2 \tag{10}$$

The initial modulus has been found to vary with the confining pressure:

$$E_i = Kp_a \left(\frac{\sigma_3}{p_a}\right)^n \tag{11}$$

where  $p_a$  is the atmospheric pressure,  $K$  and  $n$  are constants to be determined.

The complete relation then becomes:

$$E_t = Kp_a \left(\frac{\sigma_3}{p_a}\right)^n \left[1 - \frac{R_f(1 - \sin\phi)(\sigma_1 - \sigma_3)}{2c \cos\phi + 2\sigma_3 \sin\phi}\right]^2 \tag{12}$$

The PGroupN analysis adopts a non-linear model, which follows the well-established hyperbolic relationship between stress and strain proposed by Duncan and Chang (1970) and also applied to pile problems by Poulos (1989). This simple relationship assumes that the soil Young's modulus ( $E_i$ ) varies with the stress level at the pile-soil interface, i.e. it is a function of the initial tangent soil modulus ( $E_i$ ), the hyperbolic curve-fitting constant ( $R_f$ ), the current pile-soil stress ( $t$ ) and the limiting value of pile-soil stress ( $\tau_{lim}$ ), as shown in Figure 5. The hyperbolic curve fitting constant  $R_f$  defines the degree of non-linearity of the stress-strain response and can range between zero (an elastic-perfectly plastic response) and one (an asymptotic hyperbolic response in which the limiting pile-soil stress is never reached). The best way to determine the value of  $R_f$  is by fitting the PGroupN load-deformation curve with the data from the full-scale pile load test. In the absence of any test data, the value of  $R_f$  can be initially estimated based on experience.

d) Soil Domain

The BEM involves the integration of an appropriate elementary singular solution for the soil medium over the surface of the problem domain, i.e. the pile-soil interface. With reference to the present problem, the well-established solution of Mindlin (1936) for a point load within a homogeneous, isotropic elastic half space has been adopted, yielding:

$$\{u_s\} = [G_s]\{t_s\} \tag{13}$$

Where  $\{u_s\}$  are the soil displacements,  $[G_s]$  is the flexibility matrix obtained from Mindlin's solution and

$\{t_s\}$  are the soil tractions. The singular part of the  $[G_s]$  matrix is calculated via analytical integration of the Mindlin functions.

#### e) Pile Domain

If the piles are assumed to act as simple beam-columns which are fixed at their heads to the pile cap, the displacements and tractions over each element can be related to each other via the elementary beam theory, yielding:

$$\{u_p\} = [G_p]\{t_p\} + \{B\} \quad (14)$$

Where  $\{u_p\}$  are the pile displacements,  $\{t_p\}$  are the pile tractions,  $\{B\}$  are the pile displacements due to unit boundary displacements and rotations of the pile cap, and  $[G_p]$  is the matrix of coefficients.

#### f) Solution of the System

The above soil and pile equations are coupled via compatibility and equilibrium constraints at the pile-soil interface. Thus, by specifying unit boundary conditions, i.e., unit values of vertical displacement, horizontal displacement and rotation of pile cap, these equations are solved, thereby leading to the distribution of stresses, loads and moments in the piles for any loading condition.

#### g) Extension to Non-linear Soil Behavior

Non-linear soil behavior is incorporated, in an approximated manner, by assuming that the soil Young's modulus varies with the stress level at the pile-soil interface (Basile, 2003). A simple and popular assumption is to adopt a hyperbolic stress-strain relationship, in which case the tangent Young modulus of the soil  $E_t$  may be written as (Duncan and Chang, 1970; Poulos, 1989):

$$E_t = E_i \left( 1 - \frac{R_f t}{t_{lim}} \right)^2 \quad (15)$$

Where  $E_i$  is the initial tangent soil modulus,  $R_f$  is the hyperbolic curve-fitting constant,  $t$  is the pile-soil shear stress, and  $t_{lim}$  is the limiting value of the pile-soil stress.

Thus, the boundary element equations described above for the linear response are solved incrementally using the modified values of soil Young's modulus of Equation (15) and enforcing the conditions of yield, equilibrium and compatibility at the pile-soil interface.

Different values of  $R_f$  should be used for the axial response of the shaft and base, and for the lateral response of the shaft. For the axial response of the shaft, there is relatively small amount of nonlinearity, and values of  $R_f$  in the range 0-0.5 are appropriate, (Poulos, 1989). The axial response of the base is highly

nonlinear, and the value of  $R_f$  in the range 0.9-0.99 is recommended (Poulos, 1989).

#### h) General Description of the Problem

Group behavior is very complex. The response of each pile is modified by the stress condition imposed on the soil by other members of the group. Therefore, the behavior is generally dependent on the pile spacing and length, relative stiffness of the piles, number of piles in the group, in addition to the soil conditions.

In order to carry out parametric study and investigate the influence of these parameters on the behavior of the piles, it is essential to start with basic problems. The problem which is chosen to be studied is a system of pile group under axial load.

Two sets of pile groups consisting of 4 and 9 piles with circular cross sections are embedded in the soil. These pile groups were assigned different internal and external variables in order to study the behavior of the piles. The internal variables refer to pile diameter, pile length and spacing between piles, while the external variables refer to the applied load, soil types and their thickness.

It is assumed that the pile cap is fully rigid and not in contact with soil. The free-standing length, which represents the distance from the ground surface to the bottom of the cap, is assigned to be 0.5 m. This means that embedded length is reduced by 0.5 m and the interface elements are not considered within this gap. Unlike the 4 pile group, the behavior of a single pile in a group of 9 piles is associated with its location within the group. The key of identification of the piles in that group is shown in Figure 6.

The soil is assumed to be homogeneous and its parameters are based on subsoil idealization. The soil layer rests on a rigid base. The level of water table is 1.0 m below the ground surface. The piles are not based on the rigid layer which classified them as floating piles. A simple idealization of the pile-soil system is shown in Figure 7.

#### i) Parametric Study

Any designer is normally interested in the following aspects of the behavior of the pile groups:

- Evaluation of the collapse load;
- Calculation of the settlement which leads to select a suitable factor of safety in the design; and
- The distribution of stress along the piles so that it can provide adequate reinforcement in the piles.

The above targets with their simple statements represent a summary for the long analysis journey through many parameters which affect the pile group behavior. Some of these parameters adopted in this study are those incorporated with the nonlinear analysis based on the BEM. Table 1 shows an outline of the analysis program for the pile group problem.

#### j) Pile Length

The length of the pile (L) plays an important role in increasing the bearing capacity of the group. The analysis begins with a pile length of 10 m and reaches a length of 25 m with increments of 5 m.

#### k) Pile Diameter

It is well known that the pile cross sectional area affects the capability of pile to sustain the loads. This parameter is taken into account during the analysis of the pile with its circular cross section. Six diameters are chosen to be the cases under study represented by (0.5 m, 0.6 m, 0.7 m, 0.8 m, 0.9 m and 1.0 m), respectively.

#### l) Spacing between Piles

Due to pile-soil-pile interaction, the group of piles tends to settle more than a proportionally loaded single pile. This is because neighboring piles are within each others, so each pile interacts with the surrounding piles which transfer the stresses to the other piles (Basile, 2003). Thus, the spacing between piles (S) is chosen as another parameter in this study. The spacing is usually correlated with the pile diameter, so the values of spacing are  $S=2D$ ,  $S=3D$ ,  $S=4D$  and  $S=5D$ .

#### m) Applied Axial Load

The failure of pile groups under axial loading has been extensively examined (Basile, 2003). The applied load is increased gradually until the stresses along the pile reach the limiting state.

#### n) Soil Type

The soil type is sand taken from Kerbala city in Iraq with the properties determined by Ghalib, (1975). The sand was washed between the No.30 (0.59 mm) and No.50 (0.297 mm) sieves to obtain a more uniform material which would not segregate during sample preparation. A special drained triaxial test on a cylindrical sand samples (76 mm height and 76 mm diameter) was used. The axial force was increased up to an axial strain of 20%. The maximum void ratio was obtained by slowly pouring a sample of the dry sand into a Proctor mould from very low height. Minimum void ratio was determined by fabricating the sand in the mould under (0.141 kg/cm<sup>2</sup>) surcharge as specified by the ASTM standards. The triaxial chamber was first filled with de-aired water, and then the soil specimen was first consolidated to equilibrium under all around confining pressure. The confining pressures were 100, 150 and 250 kN/m<sup>2</sup>. Volumetric changes were measured during the application of the cell pressure. Table 2 illustrates the properties of the soil to be considered in this study. The stress – strain curves from triaxial test are shown in Figure 8.

This sand was used in this simulation because it has good properties and detailed tests on this sand are well documented.

#### o) Soil Thickness

The groups of piles are embedded in a soil layer with a thickness (H) of 30 m, 45 m, 60 m and 75 m

respectively, in order to study the effect of soil layer thickness. The program shows incapability to deal with cases where the pile is standing directly upon the bottom rigid layer (i.e.  $H=L$ ).

### III. RESULTS AND DISCUSSION

The results were normalized by taking the factor  $K_p$  (stiffness factor) represented by the equation:

$$K_p = \frac{P}{GWD} \quad (16)$$

Where  $P$  = axial load,

$$G = \text{shear modulus of the soil medium} = \frac{E}{2(1+\nu)}$$

$W$  = displacement of head of pile, and

$D$  = shaft diameter.

The non-dimensional stiffness factor ( $K_p$ ) for 4 pile group embedded in sand is shown in Figures 9 to 11 as a function of the length to diameter ratio (L/D). This factor gives an indication to the load-settlement relationship during the loading process. Since the cap is assumed to be fully rigid, thus all the piles in the group settle by the same amount. The piles are arranged at different spacing for each load increment to find out their effects on the group behavior.

It is well known that increasing the pile length means that more shaft resistance is generated at the pile-soil interface along its length; moreover, the pile is penetrating the soil to settle down on a stiffer stratum. This increase in the pile capacity, if the load is still the same, leads to a reduction in the group settlement which is clearly shown in these figures. At an applied load of (8000 kN), Figure 9 checks that an increase in the pile length from (10 m) to (25 m) results in 53% decrease in settlement, whereas this percentage becomes 63% as the load increases up to 12000 kN. One can also notice the loss of the first points (i.e. at  $L=10$  m) in some figures. This means that as the applied load is continuously increased, the shorter piles will be failed first.

These figures also show the role of the pile diameter during the loading process. The enlargement of the pile diameter produces a reduction in the intensity of loads carried by each pile in the group. The result is a reduction in loads to be transferred to the soil and less settlement is to be produced.

Figures 9 to 11 also show the influence of spacing between piles in a group. The behavior of a single pile in the group is associated with the others by means of strong bond, which is the cap. Thus, as the distance between the neighboring piles decreases, the interaction between these adjacent piles increases and vice versa. The results indicate that settlement of the short pile of a length (10 m) is decreased by 11% due to

doubling the spacing from ( $S=2D$ ) to ( $S=4D$ ) while for pile of a length (25 m), the doubling process did not make a considerable effect.

Figure 12 shows the effects of the presence of a pile within a group as compared with a single pile having the same properties and dimensions. It is clearly shown that the interaction between piles in a group tends to increase the settlement more than the single pile even if they carry the same amount of loads.

Figure 13 shows the variation of the skin friction along a single pile in the group. Here, the pile length is chosen to be (25 m) and the friction at the pile interface is taken as the accumulative forces along the pile length. In close examination of this figure, one can notice the high convergence among the curves at each pile diameter. This gives an impression that the frictional resistance at the shaft is developed first until it reaches the limiting stress, then the pile base will take the rest of the applied load.

It is evident that the shaft resistance increased with increasing pile diameter due to the increase in the surface area which is in contact with the surrounding soil. This will contribute in a more frictional resistance to be added to the pile capacity with each diameter increment. The direct relation with depth reflects the influence of the effective overburden stress which increases with depth.

Figure 14 shows the corresponding plots of the percentage of load carried by the pile base. For a group of 4 piles and connected with a square cap, the load on each pile is equal since the total load is applied axially at the center of group. The miscellaneous trends of the curves from the linear to nonlinear and, return back finally to the linear path indicate the sharing process between the shaft and the base of the pile. The middle portion of the curves illustrates the beginning of the shaft resistance to take its share of the total load until it is fully mobilized.

This feature is compatible with the load-settlement curves shown in Figure 15. The nonlinear path is approximately diminished as the pile reaches its ultimate bearing capacity.

Figures 16 to 18 show the plot of the non-dimensional stiffness ( $K_p$ ) as a function of pile depth. These relations are given for 9 pile group embedded in sand and subjected to sequence of axial loads applied at the center of the cap. Generally, the curves follow similar trends as in the case of 4 pile group during the variation of different parameters. Although the two mentioned series of the pile groups have similar trends but they are different in their values. The results are in good agreement with those of Butterfield and Banerjee (1971 b) and Paiva and Trondi (1999).

As a supplement to these figures, Figure 19 shows the relation of the pile head settlement against the total applied load for 9 pile group embedded in

sand. A comparison with the load-settlement curves of 4 pile group shown in Figure 15 clarifies the influence of increasing the number of piles in the group in causing a larger amount of settlement. This result makes sense because as the number of piles in the group increases with constant spacing, the interaction between the adjacent piles certainly increases and the effects are more pronounced.

A rigid cap commonly offers uniform displacements for the group, but, on the other hand, a nonuniform distribution of loads appears. This fact is clearly shown in Figure 20 which indicates the load distribution on group of 9 piles embedded in sand. The load on each pile ( $P$ ) is normalized by the average load of all piles in the group ( $P_{av}$ ). It is evident that the greatest loads are carried out by the corner piles, followed by the border piles (mid-side piles) and the center pile which is compatible with Basile (2003) and Matos et al. (2005). The reason is that the center pile, due to pile-soil-pile interaction, will need a smaller amount of load to settle of the same amount as the corner pile. It can be seen that the corner pile carries about 4% more than the average load, while the border and the center piles carry 2% and 10% less than the average load, respectively. As the ratio of pile spacing to diameter ( $S/D$ ) increases, the difference between loads on each pile decreases, especially between the corner and the center piles.

One can find a noticeable effect of the pile spacing to diameter ratio ( $S/D$ ) on the load distributed for all the piles in the group but for the border pile. As the spacing ratio increases from ( $S/D=2$ ) to ( $S/D=5$ ), the difference between the corner and the center piles is reduced from 13% to 6% with approximately a horizontal path for the border piles. At a spacing ratio ( $S/D=3$ ), the effect of length seems to be diminished through the high convergence between the different lengths behind this ratio. This refers to that moving the pile apart from the adjacent piles in a group tends to reduce the interaction among them which allow the pile to go through more independence.

Ideally, for an axially loaded pile group, all piles will carry the same amount of load as the total applied load approaches the ultimate load capacity of the group (Basile, 2003). This feature becomes clearer in Figure 17 as the total load increases towards its ultimate value.

Figure 21 illustrates the share of load carried by the base of each pile in the group. It can be seen that the pile's base takes different portions of loads according to their locations but follow the same trend during the gradual increase in the applied load. This may lead to think, as it was mentioned before in the problem of 4 pile group, that the shear stress along the pile's interface is developed equally regardless of the number and location of piles.

#### IV. CONCLUSIONS

1. A rigid cap offers uniform displacements for all the piles in the group, but on the other hand, a non uniform distribution of loads appears. For the group of 9 piles, the maximum loads are carried by the corner piles, followed by the border piles and the center piles. This conclusion obtained by the boundary element analysis coincides with the same findings obtained by other approaches.
2. For 9 pile group analyzed, the corner pile carries about 4% more than the average load, while the border and the center piles carry 2% and 10% less than the average load, respectively. As the ratio of pile spacing to diameter (S/D) increases, the difference between loads on each pile decreases, especially between the corner and the center piles.
3. As the applied load reaches the ultimate capacity of the group, all the piles will share the same amount of load.
4. For a pile group embedded in sand, the shear stress along the pile interface increases gradually during the loading process until it become fully mobilized, then the pile base takes the rest of the applied load. This shear stress is found to be equally developed regardless of the number and the location of the piles in the group.

#### REFERENCES RÉFÉRENCES REFERENCIAS

1. Banerjee, P.K. and Butterfield, R., (1981), "Boundary Element Method in Engineering Science", McGraw - Hill, London.
2. Basile, F., (2003), "Analysis and Design of Pile Groups", in: "Numerical Analysis and Modeling in Geomechanics", edited by J.W. Bull, Spon Press, London, p.p. 278-315.
3. Beer, G., (1986), "Implementation of Combined Boundary Element-Finite Element Analysis with Applications in Geomechanics", in: Developments in Boundary Element Methods-4, edited by P.K. Banerjee, and J.O. Watson, Elsevier Applied Science Publishers, LTD.
4. Beer, G. and Watson, J.O., (1992), "Introduction to Finite and Boundary Element Methods for Engineers", John Wiley& Sons, Chichester.
5. Butterfeild, R. and Banerjee, P.K., (1971a), "The Elastic Analysis of Compressible Piles and Pile Groups", *Geotechnique*, Vol.21, No.3, p.p. 43 – 60.
6. Butterfeild, R. and Banerjee, P.K., (1971b), "The Problem of Pile Group- Pile Cap Interaction", *Geotechnique*, Vol.21, No.2, p.p.135-142.
7. Chang, C.Y. and Duncan, J.M., (1970), "Analysis of Soil Movement around a Deep Excavation", *Journal of Soil Mechanics and Foundations Division, ASCE*, Vol.96, No.SM5, p.p.1655-1681.
8. Chin, J.T., (2004), "Single Pile Settlement: A Practical Assessment", 15th Southeast Asian Geotechnical Society Conference, Bangkok, Thailand.
9. Christian, J.T. and Desai, C.S., (1977), "Constitutive Laws for Geological Media", in: "Numerical Methods in Geotechnical Engineering", edited by C.S. Desai and J.T. Christian, McGraw-Hill, New York, p.p. 65-116.
10. Crouch, S.L. and Starfield, A.M., (1983), "Boundary Element Methods in Solid Mechanics", George Allen & Unwin, London.
11. Duncan, J.M. and Chang, C.Y., (1970), "The Non-Linear Analysis of Stress and Strain in Soils", *Journal of Soil Mechanics and Foundations Division, ASCE*, Vol.96, No.SM5, p.p.1629-1653.
12. Ghalib, S.A. (1975), "Stress-Strain Relations for an Iraqi Sand", M.Sc. Thesis, University of Baghdad, College of Engineering.
13. Geocentrix Ltd (2002), "Repute 1.0, Pile Group Design Software", <www. Geocentrix.co.uk> .
14. Hobbs, R. George, P.J. and Mustoe, C.G.W., (1978), " Some Applications of Numerical Methods to the Design of Offshore Gravity Structure Foundations", in: "Numerical Methods in Offshore Engineering", edited by O.C. Zeinkiwicz, R.W. Lewis, and K.G. Stagg, John Wiley& Sons, p.p.472 - 482.
15. Kondner, R.L., (1963), "Hyperbolic Stress-strain Response: Cohesive Soils", *Journal of Soil Mechanics and Foundations Division, ASCE*, Vol.89, No.SM1, p.p.115-143.
16. Lancellotta, R., (2009), "Geotechnical Engineering", second edition by Taylor & Francis.
17. Matos Filho, R. Mendonça, A.V. and Paiva. J.B., (2005), "Static Boundary Element Analysis of Piles Subjected to Horizontal and Vertical Loads", *Engineering Analysis with Boundary Elements*, Vol.29, p.p.195-203.
18. Mindlin, R.D. (1936), "Force at a point in the interior of a semi-infinite solid", *Journal of Applied Physics*, Vol. 7, No.5, p.p. 195-202.
19. Paiva, J.B. and Trondi, R.R., (1999), "Boundary Element Analysis of Capped and Uncapped Pile Groups", *Advances in Engineering Software*, Vol.30, p.p. 715-724.
20. Poulos, H.G., (1971a), "Behaviour of Laterally Loaded Piles: I – Single Pile", *Journal of Soil Mechanics and Foundations Division, ASCE*, Vol.97, No.SM5, p.p. 711 – 731.
21. Poulos, H.G., (1971b), "Behaviour of Laterally Loaded Piles: II- Pile Groups", *Journal of Soil Mechanics and Foundations Division, ASCE*, Vol.97, No.SM5, p.p.733 – 751.
22. Poulos, H.G., (1989), "Pile Behaviour – Theory and Application". 29th Rankine Lecture, *Geotechnique*, vol.39, No.3, p.p.365-415.
23. Venturini, W.S., (1983), "Boundary Element Method in Geomechanics", Springer -Verlag, Berlin.



Table 1 : Analysis program for pile group problem

Pile diameters are ranged from 0.5 m – 1.0 m with an increment of 0.1 m							
S=2D		S=3D		S=4D		S=5D	
L=10 m	H=30 m	L=10 m	H=30 m	L=10 m	H=30 m	L=10 m	H=30 m
	H=45 m		H=45 m		H=45 m		H=45 m
	H=60 m		H=60 m		H=60 m		H=60 m
	H=75 m		H=75 m		H=75 m		H=75 m
L=15 m	H=30 m	L=15 m	H=30 m	L=15 m	H=30 m	L=15 m	H=30 m
	H=45 m		H=45 m		H=45 m		H=45 m
	H=60 m		H=60 m		H=60 m		H=60 m
	H=75 m		H=75 m		H=75 m		H=75 m
L=20 m	H=30 m	L=20 m	H=30 m	L=20 m	H=30 m	L=20 m	H=30 m
	H=45 m		H=45 m		H=45 m		H=45 m
	H=60 m		H=60 m		H=60 m		H=60 m
	H=75 m		H=75 m		H=75 m		H=75 m
L=25 m	H=30 m	L=25 m	H=30 m	L=25 m	H=30 m	L=25 m	H=30 m
	H=45 m		H=45 m		H=45 m		H=45 m
	H=60 m		H=60 m		H=60 m		H=60 m
	H=75 m		H=75 m		H=75 m		H=75 m

Table 2 . Soil parameters of Kerbala sand for different models (after Ghalib, 1975)

a. Identification properties

Soil Properties	Value
Uniformity coefficient, Cu	1.41
Effective diameter, $D_{10}$	0.44 mm
Coefficient of curvature, Cc	0.36
Specific gravity, Gs	2.679
Min. void ratio, $e_{min}$	0.543
Max. void ratio, $e_{max}$	0.8043
Relative density, Dr %	80.835

b. Strength properties

Soil properties	Linear-Elastic model	Duncan and Chang model	Mohr- Coulomb model
$E_i$ (kN/m <sup>2</sup> )	124000	124000	124000
	171500	171500	171500
	220000	220000	220000
$\gamma_{bulk}$ (kN/m <sup>3</sup> )	20.15	20.15	20.15
Poisson's ratio $\nu$	0.32	0.32	0.32
$\sigma_3$ (kN/m <sup>2</sup> )	100	100	100
	150	150	150
	250	250	250
$\phi$ (degree)	-	40	40

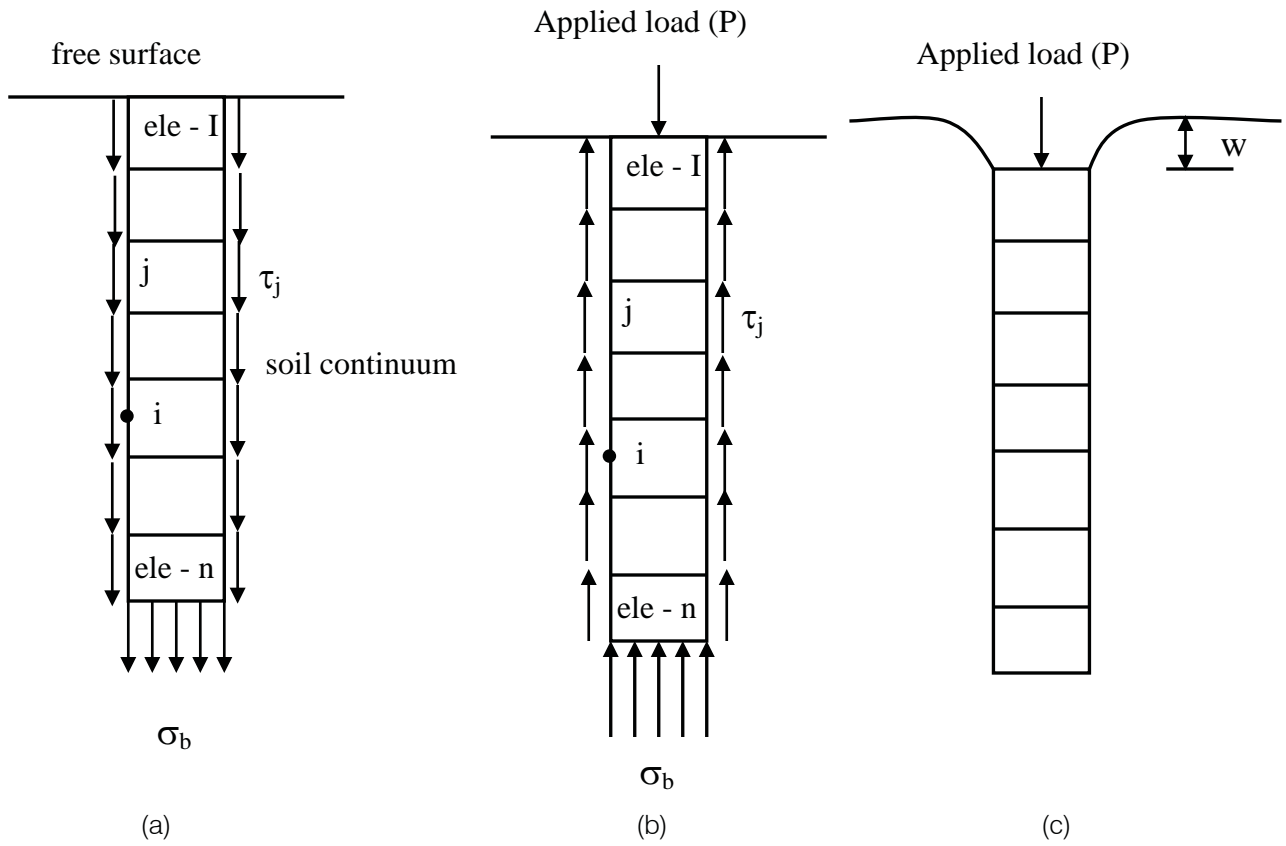


Figure 1 : Schematic diagram of the integral equation method (after Poulos, 1971a)

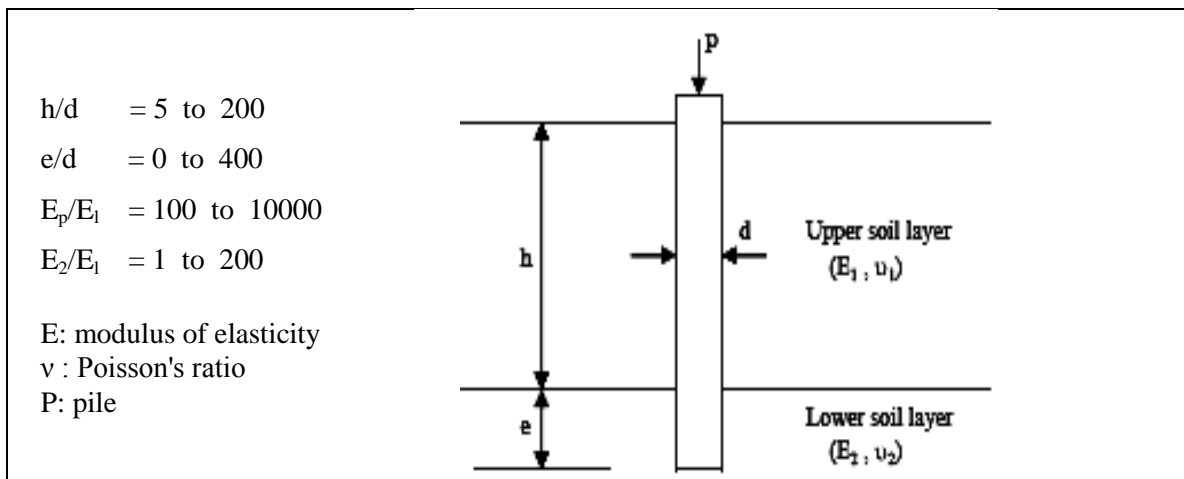


Figure 2 : Single pile problem embedded in two layers soil profile (after Chin, 2004)

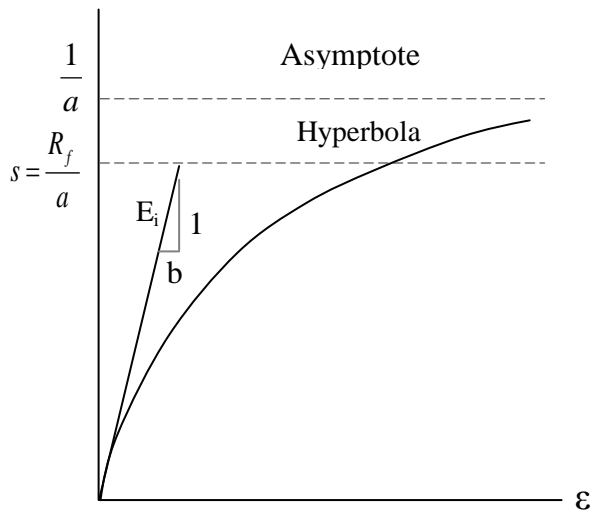


Figure 3 : Hyperbolic stress-strain curve for non-linear material (from Christian and Desai, 1977)

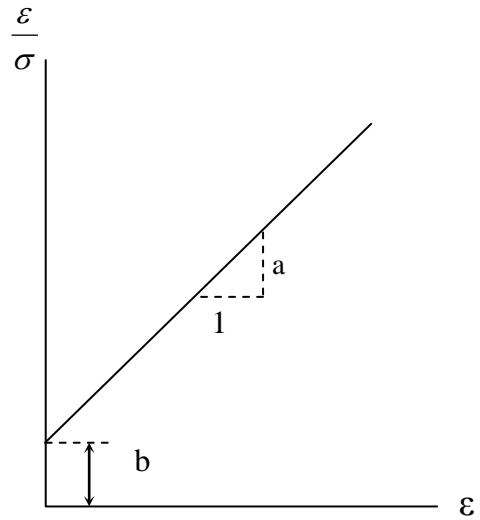


Figure 4 : Transformed hyperbolic stress-strain curve (from Christian and Desai, 1977)

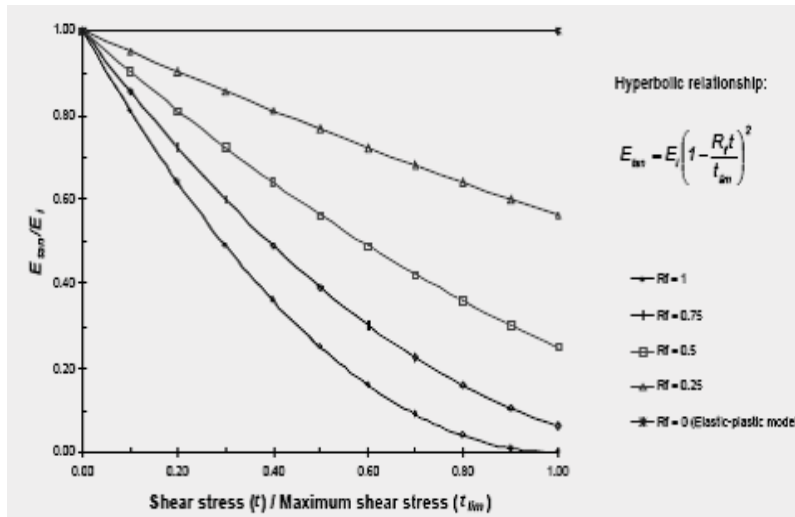


Figure 5 : Soil Young's modulus variation with stress level (from Geocentrix, 2002)

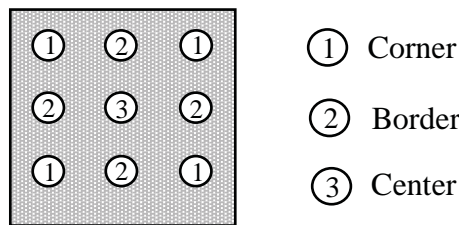


Figure 6 : Identifications of the 9 piles in the group

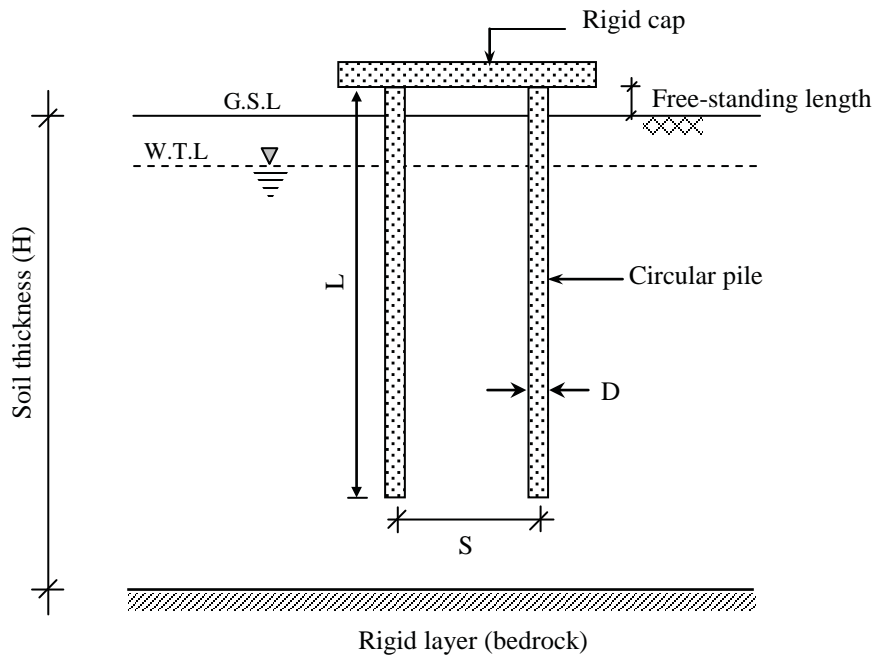


Figure 7 : The problem of pile group

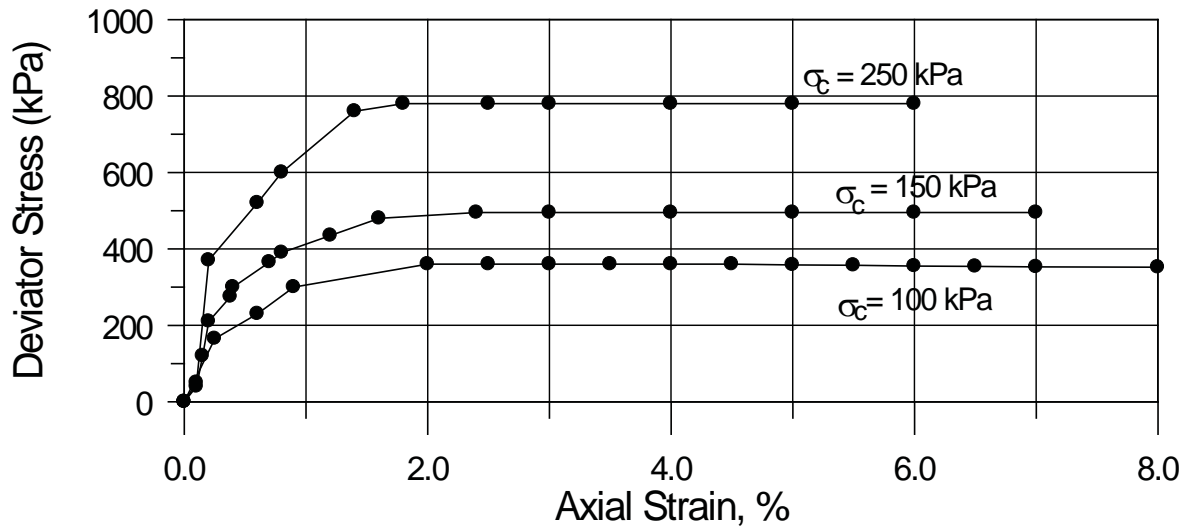


Figure 8 : Results of triaxial test (after Ghalib, 1975)

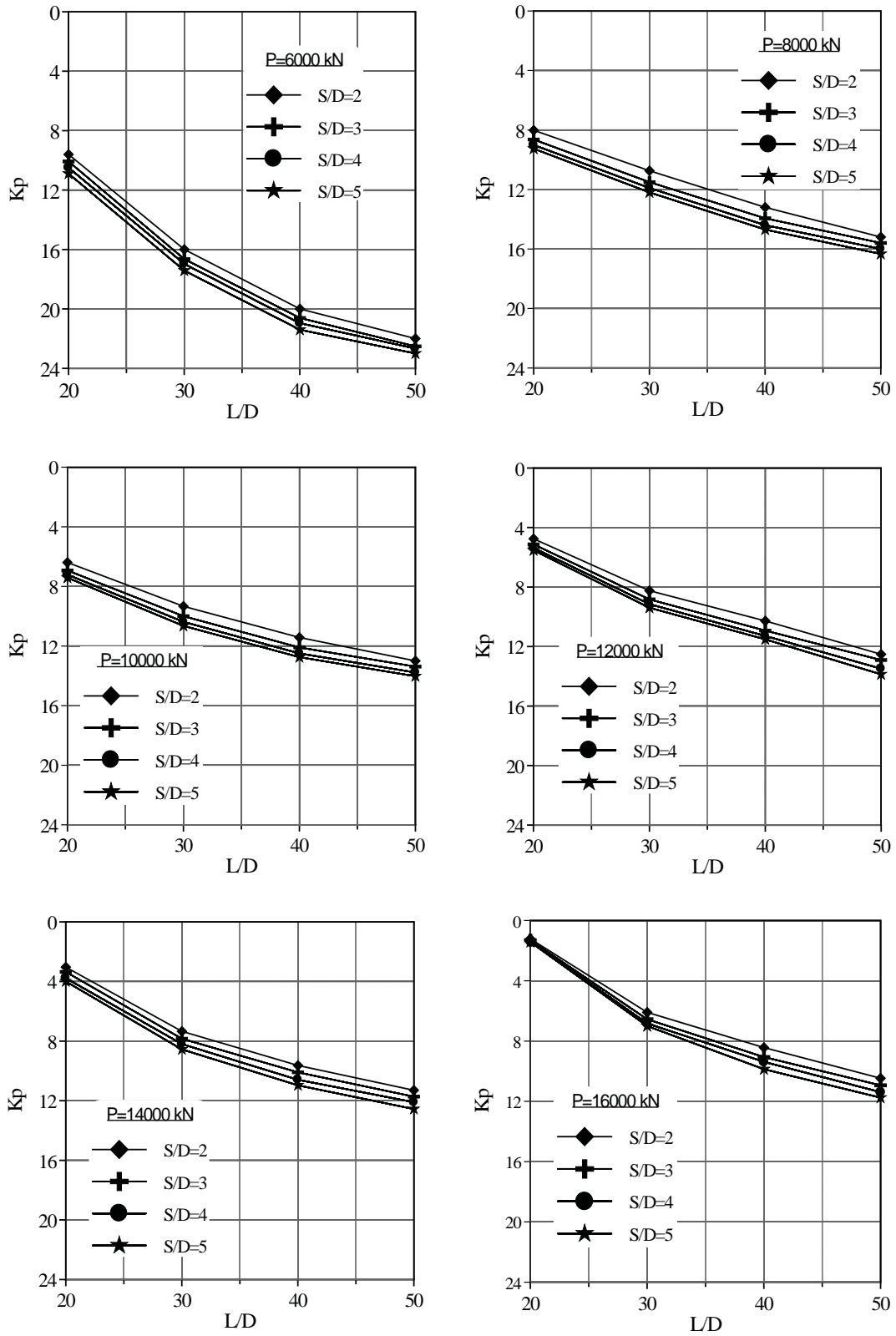


Figure 9 : Normalized load-settlement curves for (2\*2) pile group of a diameter D=0.5 m, embedded in sand

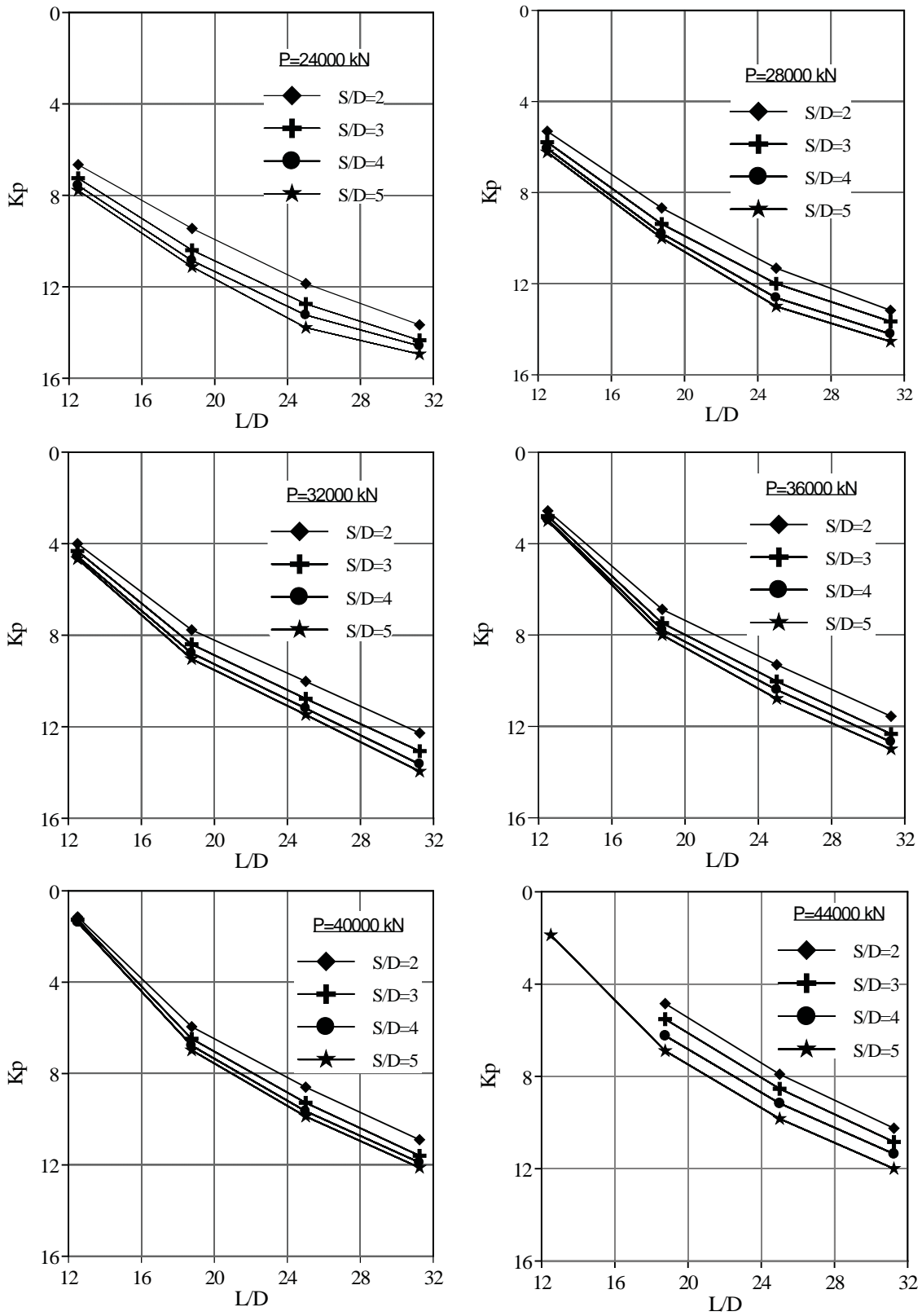


Figure 10 : Normalized load-settlement curves for (2\*2) pile group of a diameter  $D=0.8$  m, embedded in sand under different loadings

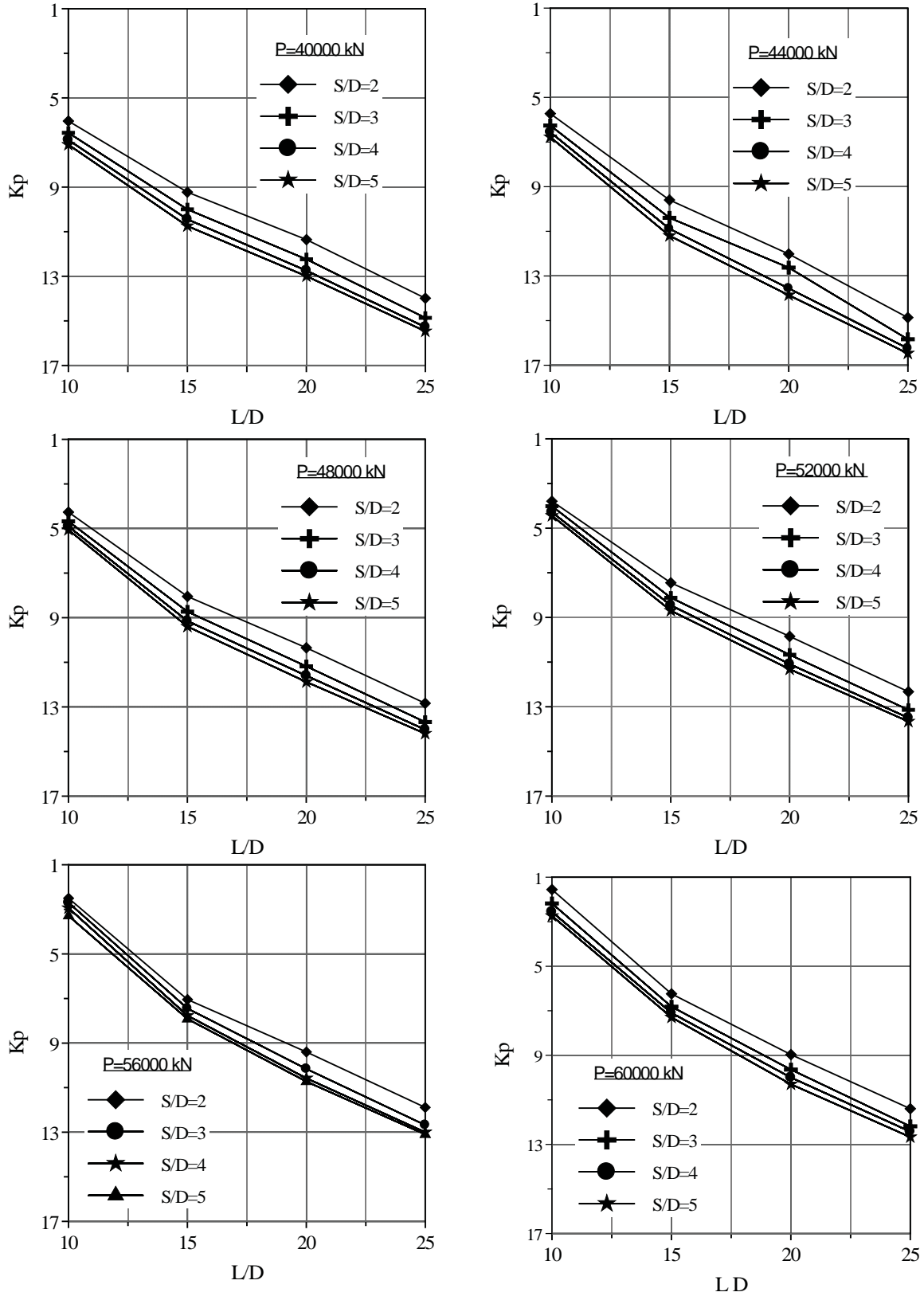


Figure 11: Normalized load-settlement curves for (2\*2) pile group of a diameter  $D=1.0$  m, embedded in sand under different loadings

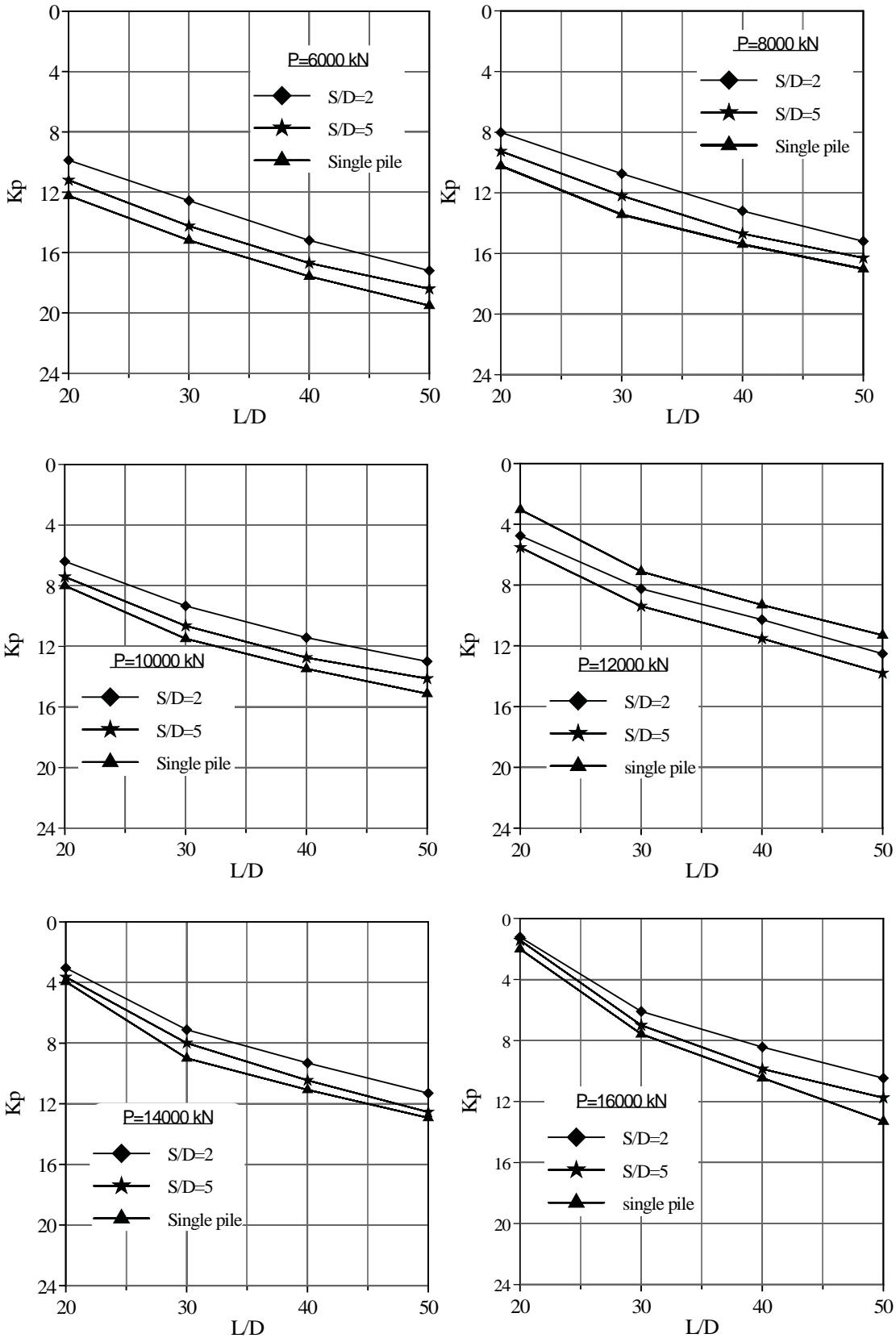


Figure 12 : Normalized load-settlement curves for (2\*2) pile group of a diameter  $D=0.5$  m, embedded in sand under different loadings as compared with a single pile



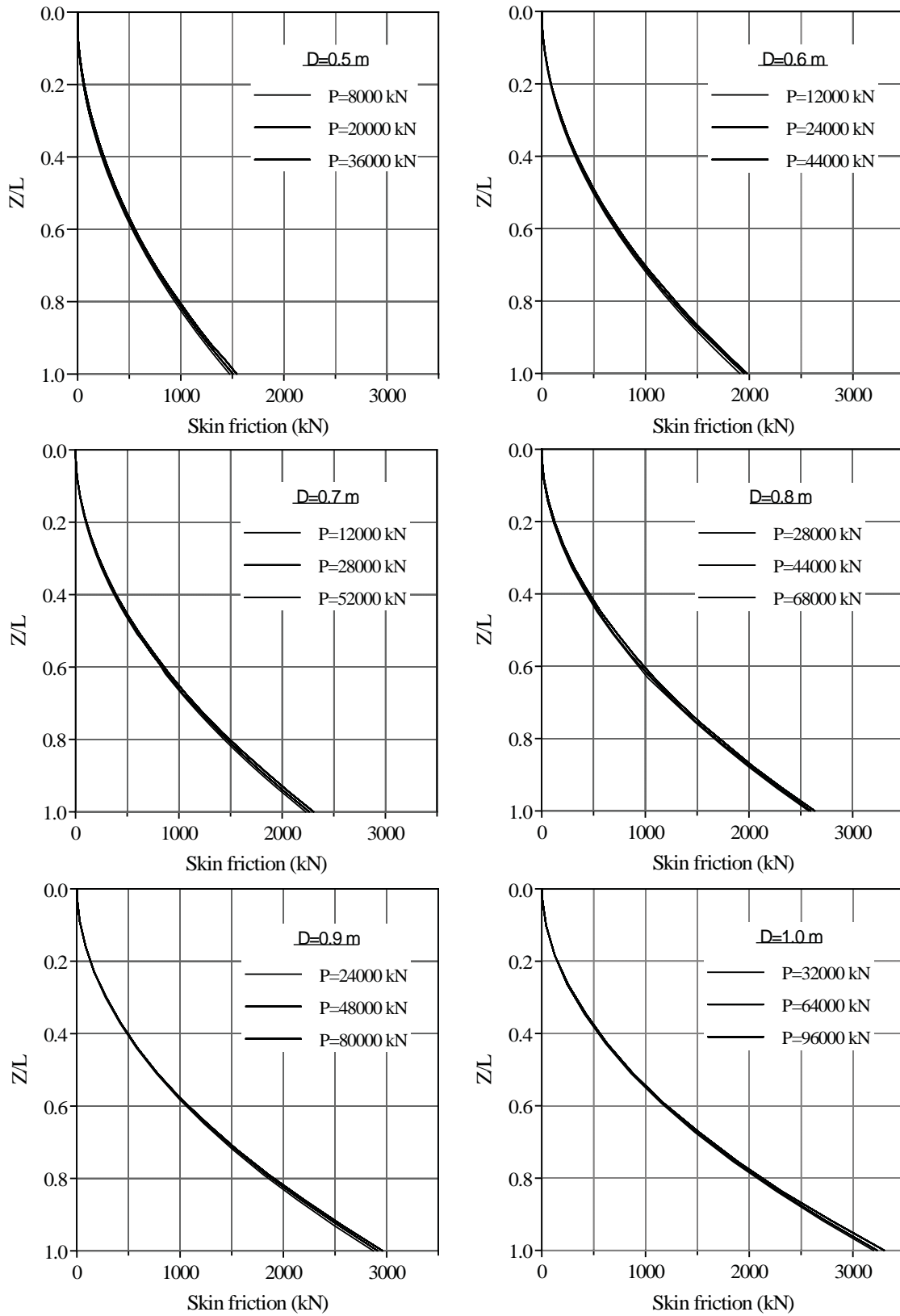


Figure 13 : Variation of skin friction along a single pile in (2\*2) pile group embedded in sand for different diameters, ( $S/D=2$ ,  $L=25\text{ m}$ )

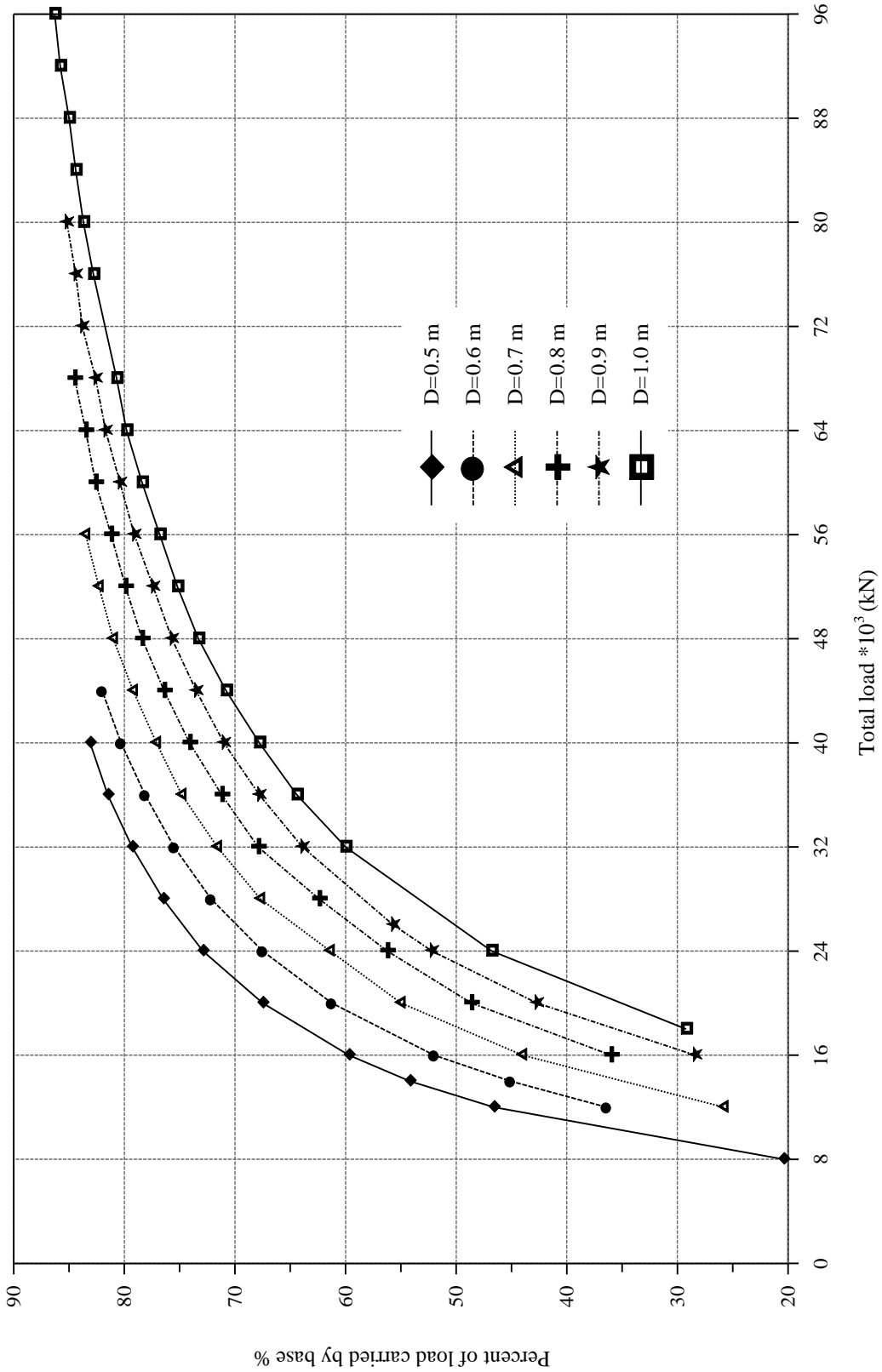


Figure 14 : Bearing force characteristics at the pile base computed as a percentage of the applied load for a (2\*2) pile group embedded in sand, (S/D=2, L=25 m)

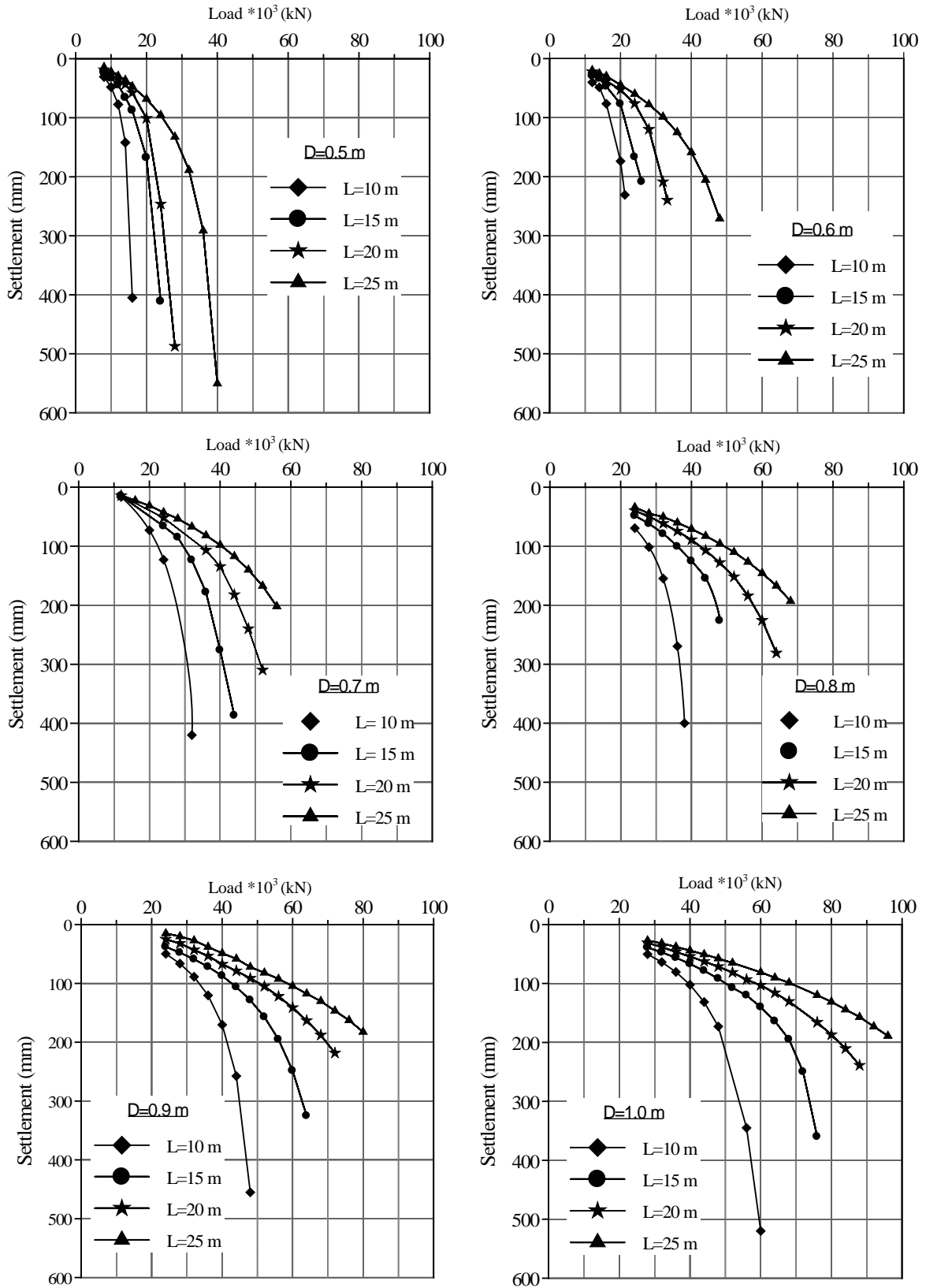


Figure 15 : Load-settlement curves for (2\*2) pile group embedded in sand (S/D=2)

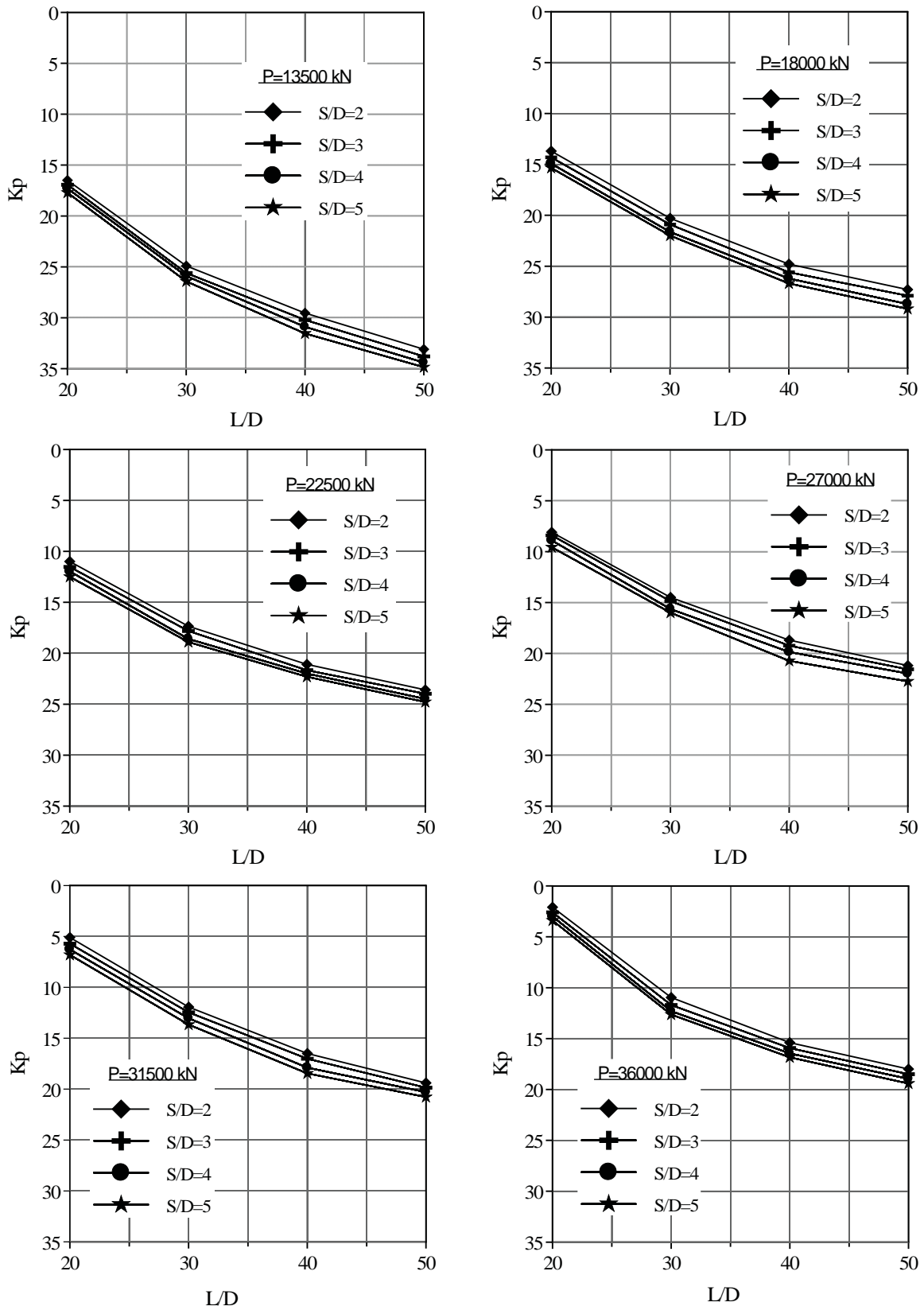


Figure 16 : Normalized load-settlement curves for (3\*3) pile group of a diameter  $D=0.5$  m, embedded in sand under different loadings

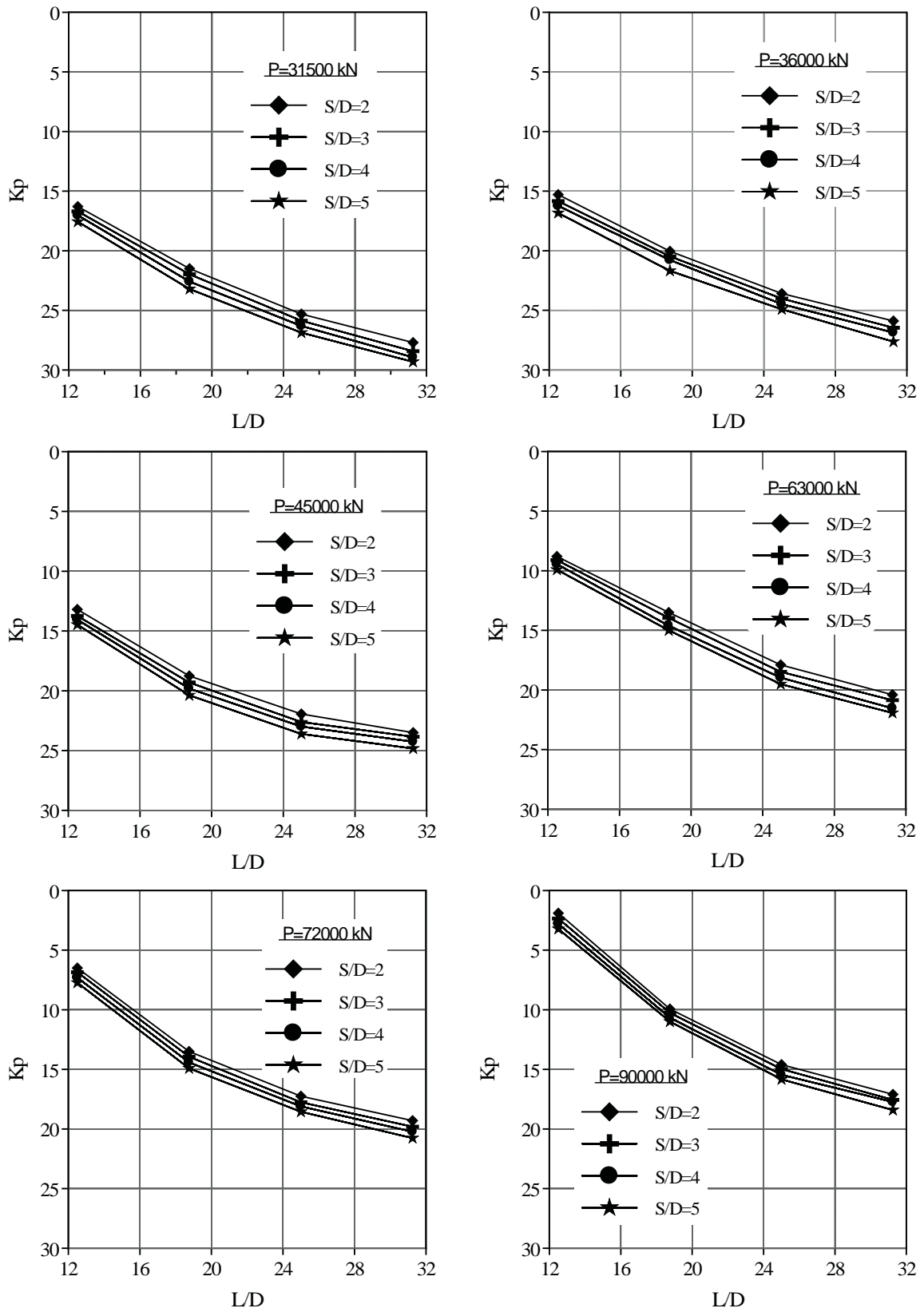


Figure 17 : Normalized load-settlement curves for (3\*3) pile group of a diameter  $D=0.8$  m, embedded in sand under different loadings

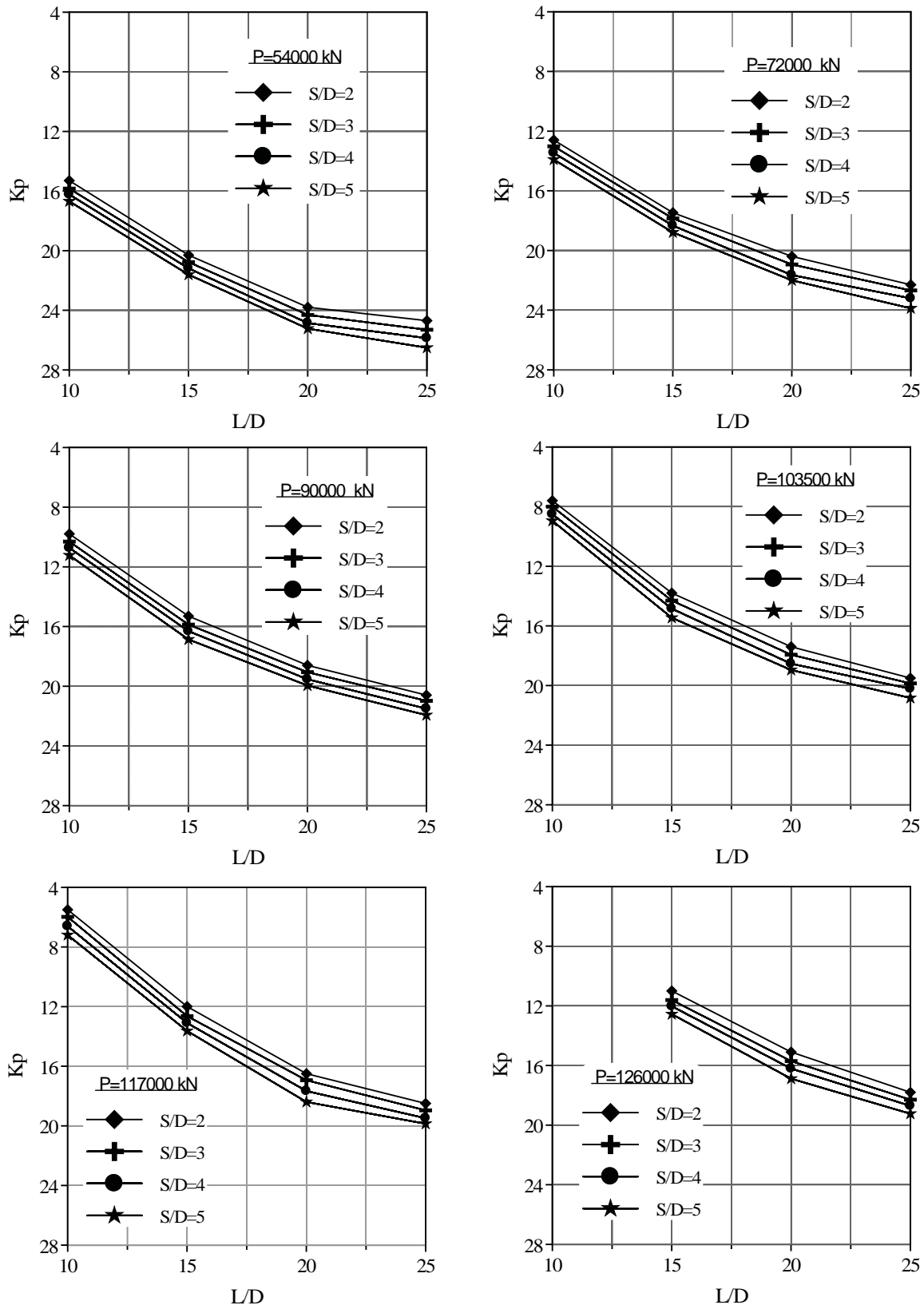


Figure 18 : Normalized load-settlement curves for (3\*3) pile group of a diameter  $D=1.0$  m, embedded in sand under different loadings

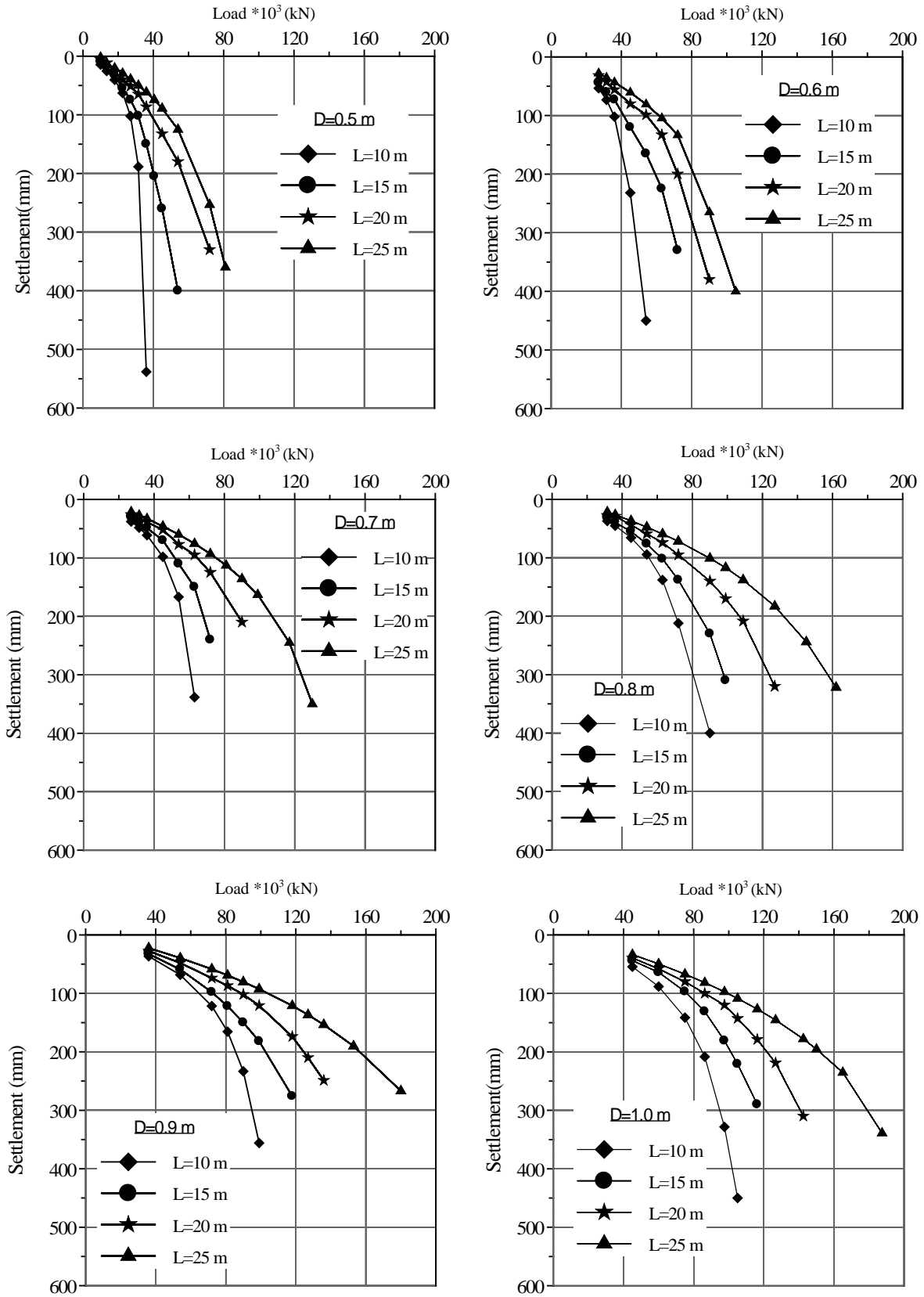


Figure 19 : Load-settlement curves for (3\*3) pile group embedded in sand, (S/D=2)

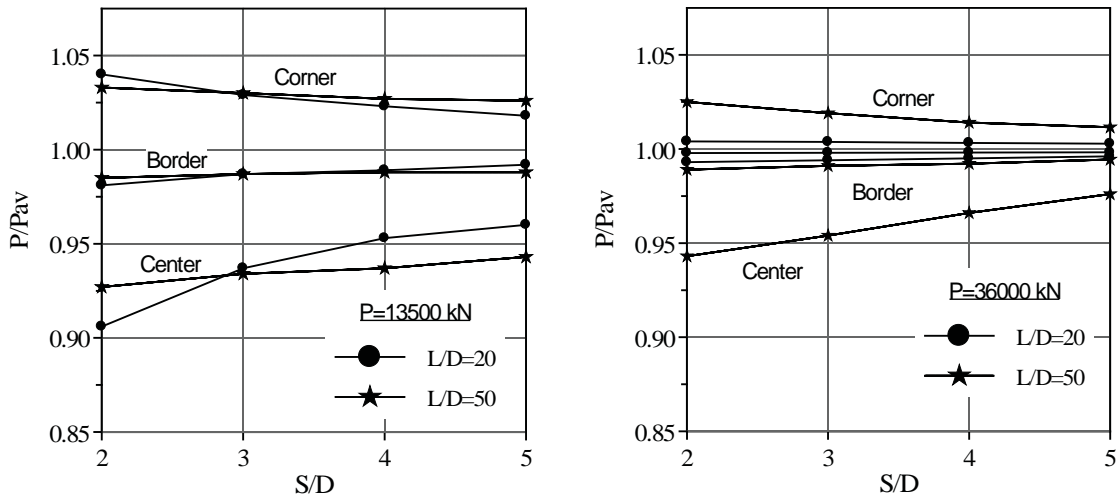


Figure 20 : Pile load distribution on (3\*3) pile group embedded in sand, (D=0.5 m)

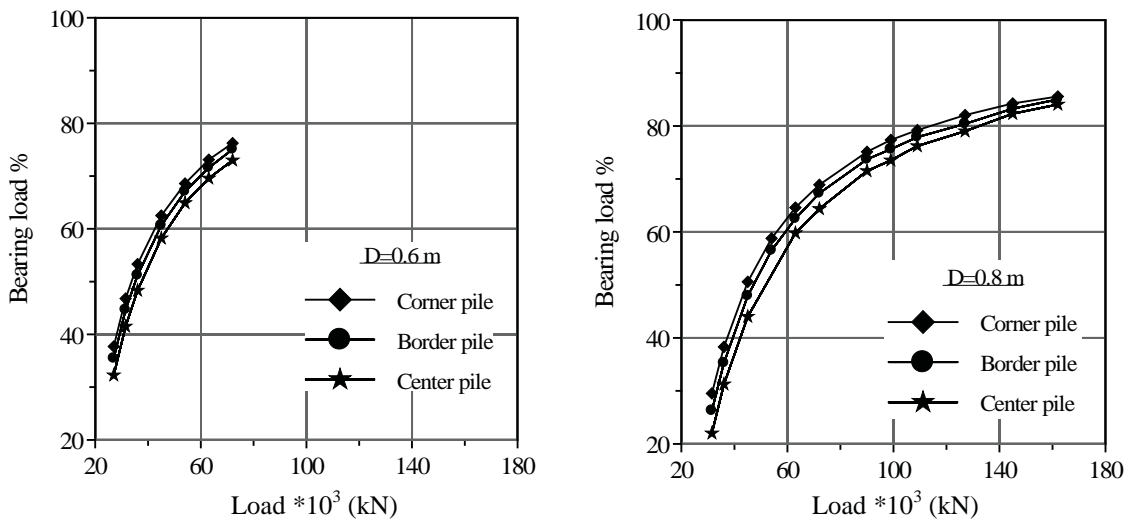


Figure 21 : Bearing force characteristics at the pile base computed as a percentage of the



This page is intentionally left blank